

Cadmium Induced Acute Lung Injury and TUNEL Expression of Apoptosis in Respiratory Cells

We examined the ultrastructural features of the lung parenchyma and the expression of apoptosis of the respiratory cells by TUNEL technique. Male Sprague-Dawley rats (n=30) were intra-tracheally injected with cadmium (2.5 mg/kg) into both lungs. The light and electron microscopic features of the lung tissues were examined on Days 1, 3, 7 and 10 after the injection of cadmium. Specimen preparations for the light and electron microscopic TUNEL stains were performed. Ultrastructurally, on Days 1 and 3, the alveolar spaces were filled with edematous fluid, and desquamated type I epithelial cells. On Days 7 and 10, the alveolar spaces and interstitium were patchy infiltrated with young fibroblasts and some collagen deposition. The light microscopic TUNEL stain showed that apoptosis of the alveolar cells was most prominent on Day 1, and then the number of apoptosis was markedly decreased on Days 3, 7 and 10. The electron microscopic TUNEL stain showed the electron dense homogenous nuclear expression, and the formation of intranuclear blebs which protrude to the outside of nuclei. On Days 7 and 10, there are frequent apoptotic nuclear bodies in the alveolar macrophages. We could examine the identification of the equivocal apoptotic cells and various morphologic expression of apoptotic nuclei on the electron microscopic TUNEL stain.

Key Words : Cadmium; Acute Lung Injury; TUNEL; Apoptosis

Kun-Young Kwon, Jae-Hwi Jang,
Sun-Young Kwon, Chi-Heum Cho*,
Hoon-Kyu Oh, Sang-Pyo Kim

Departments of Pathology, Obstetric and Gynecology*,
Keimyung University School of Medicine, Daegu, Korea

Received : 19 May 2003
Accepted : 24 July 2003

Address for correspondence

Kun-Young Kwon, M.D.
Department of Pathology, Keimyung University School
of Medicine, 194 Dongsan-dong, Choong-gu, Daegu
700-712, Korea
Tel : +82.53-250-7482, Fax : +82.53-250-7852
E-mail : k19156ky@dsmc.or.kr

*This work was supported by the research promoting
grant from the Keimyung University Dongsan Medical
Center in 1999.

INTRODUCTION

Apoptosis not only plays a critical role in normal physiological processes, but can also be important for many of the pathological consequences of diseases (1, 2). Inhalation of cadmium can cause emphysema, pulmonary fibrosis, and even carcinomas in human and experimental models (3-5). The mechanisms of the diverse pathologic lesions by the cadmium are, however, not well established. In the literatures, there have been several reports of cadmium-induced apoptosis in vitro studies (6-8), and in vivo studies of kidney (9), testis (10) and liver (11). But only a few studies related with apoptosis in the cadmium-induced acute lung injury in vivo were reported (4, 12).

In situ terminal deoxynucleotidyl transferase mediated dUTP nick end labeling (TUNEL) method has proven to be a convenient and reproducible method to detect the 3'-OH ends of cleaved DNA in apoptotic cells in the frozen, fresh and formalin-fixed paraffin embedded tissues (13). The standard protocol for electron microscopic TUNEL method has not been fully established. This study was designed to examine the ultrastructural features of the intra-tracheally cadmium injected lung parenchyma and the expressions of apoptosis of the respiratory epithelial cells, endothelial cells, alveolar macro-

phages, and interstitial cells by light and electron microscopic TUNEL methods.

MATERIALS AND METHODS

Thirty male Sprague-Dawley rats weighing 200-250 g were used in this study. Commercial rat feed and drinking water were offered. Animals including control rats (n=5) were acclimated for one week prior to experimentation. Experimental rats were divided into Days 1 (n=5), 3 (n=5), 7 (n=5), and 10 (n=10) after injection of cadmium. Before intra-tracheal injection of the cadmium, the animals were anesthetized with pentothal sodium (Thiopenton natorium, 250 mg/kg, intraperitoneally). The animals were incised vertically the anterior neck skin (about 1 cm), dissected the trachea carefully, inserted a 21-gauge needle, and injected cadmium chloride (CdCl₂, Sigma, St Louis, MO, U.S.A., 2.5 mg/kg) into both lungs. The experimental rats were survived all on Days 1 and 3, but four and five rats were survived on Days 7 and 10 after injection of cadmium, respectively. Specimen preparations for the light microscopic, transmission and scanning electron microscopic examinations were performed by routine procedures in all survived rats of each experimental and control groups. We

also performed the light microscopic TUNEL stains using formalin fixed paraffin embedded tissue, and the light microscopic and electron microscopic TUNEL stains using dry ice-acetone frozen tissue blocks in three rats of each group.

Light microscopic TUNEL stain using paraffin-embedded tissue

The paraffin sections were cut to 5 μm in thickness and were mounted on silane-coated glass slides, and stored for 1 hr at 60°C. The slides were deparaffinized with 3 times of xylene for 5 min each, and were rehydrated with graded alcohols (100%, 95%, 70%, and 50% alcohols for 5 min, respectively). After washing in 0.01 M phosphate-buffered saline (PBS) for 5 min, the sections were digested with Proteinase K (20 $\mu\text{g}/\text{mL}$) at room temperature for 20 min, and were washed 2 times with distilled water (DW) for 2 min each. After the endogenous peroxidase activity was blocked with 3% hydrogen peroxide (H_2O_2) in PBS for 5 min, the slides were rinsed 2 times with PBS for 5 min. For positive control, the sections which treated with 3% H_2O_2 , were reacted with DNase I (1-2 U) at 37°C for 30 min, and then washed 2 times with PBS. The slides were covered with 75 μL of terminal deoxynucleotidyl transferase (TdT) buffer for 10 min, and added 50 μL TdT/dUTP solution. The sections were covered with plastic cover slips and incubated in a moisture chamber at 37°C for 1.5 hr. For negative control, the sections were covered only with reaction buffer and incubated under the same conditions. The slides dipped into Coplin jar containing prewarmed stop buffer, agitated for 15 sec, and incubated for 10 min at 37°C, and then washed the sections in three changes of PBS for 5 min. The sections were covered with anti-digoxigenin peroxidase conjugate and incubated for 30 min at 37°C using moisture chamber. The slides were washed in 3 times of PBS for 2 min each, and were applied 100 μL of freshly prepared diaminobenzidine (DAB, DAKO, U.S.A.) solution on each section and incubated at room temperature for 3 to 5 min in the dark. The slides were washed in 3 times of DW in a Coplin jar for 1 min each with microscopic examination. The sections were lightly counterstained with hematoxylin for 1 min, washed with tap water, and dehydrated once in 70% ethanol for 3 min, once in 95% ethanol for 3 min, and twice in 100% ethanol for 5 min each time. The sections were cleared 2 times in xylene for 5 min each, removed excess xylene and mounted with Permount. On the light microscopic TUNEL stain, we counted the number of apoptotic cells and evaluated the degree of apoptosis in different experimental groups.

Light microscopic and electron microscopic TUNEL stains using dry ice-acetone frozen tissue

The lung tissues were removed from the experimental animals, and cut into small pieces ($4 \times 4 \times 1 \text{ mm}$), and fixed in 4% paraformaldehyde (PFA) in 0.01 M PBS (pH 7.4) or per-

iodate lysine paraformaldehyde (PLP) solution at 4°C overnight. After washing with 0.01 M PBS, the lung tissues were immersed in graded concentrations of sucrose in PBS (10% for 1 hr, 15% for 2 hr, 20% for 4 hr) at 4°C. Then the tissues were embedded in optimal cutting temperature (OCT) compound and frozen in a dry ice-acetone bath. The OCT-embedded tissue blocks were stored at -80°C. The frozen blocks were cut to 6 μm sections in thickness (7-9 μm sections in thickness for EM TUNEL) in a cryostat and were mounted on silane-coated glass slides. The sections were air-dried and stored at -20°C until use. After washing in 0.01 M PBS for 5 min, the sections were reacted with Proteinase K (20 $\mu\text{g}/\text{mL}$) at room temperature for 15 min, and then were washed 5 times with DW for 2 min each. The endogenous peroxidase activity was blocked with 3% H_2O_2 in methanol for 25 min, the slides were rinsed 5 times with DW for 2 min each. The sections were treated with 50 μL of TdT reaction solution for 3 hr, and stopped the TdT reaction by using $2 \times \text{SSC}$ for 15 min at room temperature, and washed in 5 times of 0.01 M PBS for 2 min each. The sections were incubated with a blocking solution containing 1% bovine serum albumin in PBS at room temperature for 20 min, and treated with peroxidase-conjugated streptavidin for 1 hr at 37°C. The slides were washed in 6 changes of 0.01 M PBS for 5 min each. The sections were reacted with Tris-HCl solution for 5 min, and were applied 100 μL of DAB solution on each section and incubated at room temperature for 3 to 5 min in the dark. The slides were washed in 5 times of 0.01 M PBS in a Coplin jar for 2 min each. For light microscopic TUNEL staining, the sections were lightly counterstained with hematoxylin for 1 min, washed with tap water, and continued the next steps of preparation for paraffin-embedded tissues. For electron microscopic TUNEL stain, the sections were reacted with 1% OsO_4 in 0.01 M cacodylate buffer for 1 hr in moisture chamber and were washed in 3 changes of 0.01 M PBS for 5 min each. The sections were then dehydrated completely with up-graded ethanols, and embedded in inverted polyethylene embedding capsules filled with PolyBed mix resin (Poly/Bed 812, Polysciences Inc., U.S.A.), which were polymerized at 60°C for 3 days. We removed the gelatin capsules from the glass slide, performed the light microscopic examination, and selected the portion of electron microscopic examination. After trimming the PolyBed mix resin blocks, ultrathin section (100 nm) was performed, and electron microscopic TUNEL stain was observed on Hitachi H-7100 electron microscope at 75 kV with no staining of uranyl acetate and lead citrate. On the electron microscopic TUNEL stain, we examined the identification of apoptotic cells and various morphologic expression of the apoptotic nuclei in the different stages of the apoptosis. We interpreted it was positive expression of TUNEL stain that the injured respiratory cells showed electron density in the nuclei of the apoptotic cells.

RESULTS

Light microscopic examination

In control group, the alveoli were generally intact, and architectural integrity of the alveoli was well preserved except scarce cellular infiltration into some alveoli. The lungs observed on Day 1 after cadmium injection show mild diffuse inflammatory changes with some neutrophilic infiltration, edema and

fibrin materials in the alveoli. On Day 3 after the injection of cadmium, several patchy inflammatory infiltration of peribronchiolar portions was seen; but neutrophilic infiltration was relatively subsided. The alveoli in the patchy lesions were filled with desquamated epithelial cells, neutrophils, fibrin materials and alveolar macrophages. On Day 7 after the injection of cadmium, multiple, patchy, and peribronchiolar consolidation was more prominent compared to the lungs observed on Day 3. Some early fibrotic plugs were found in the bron-

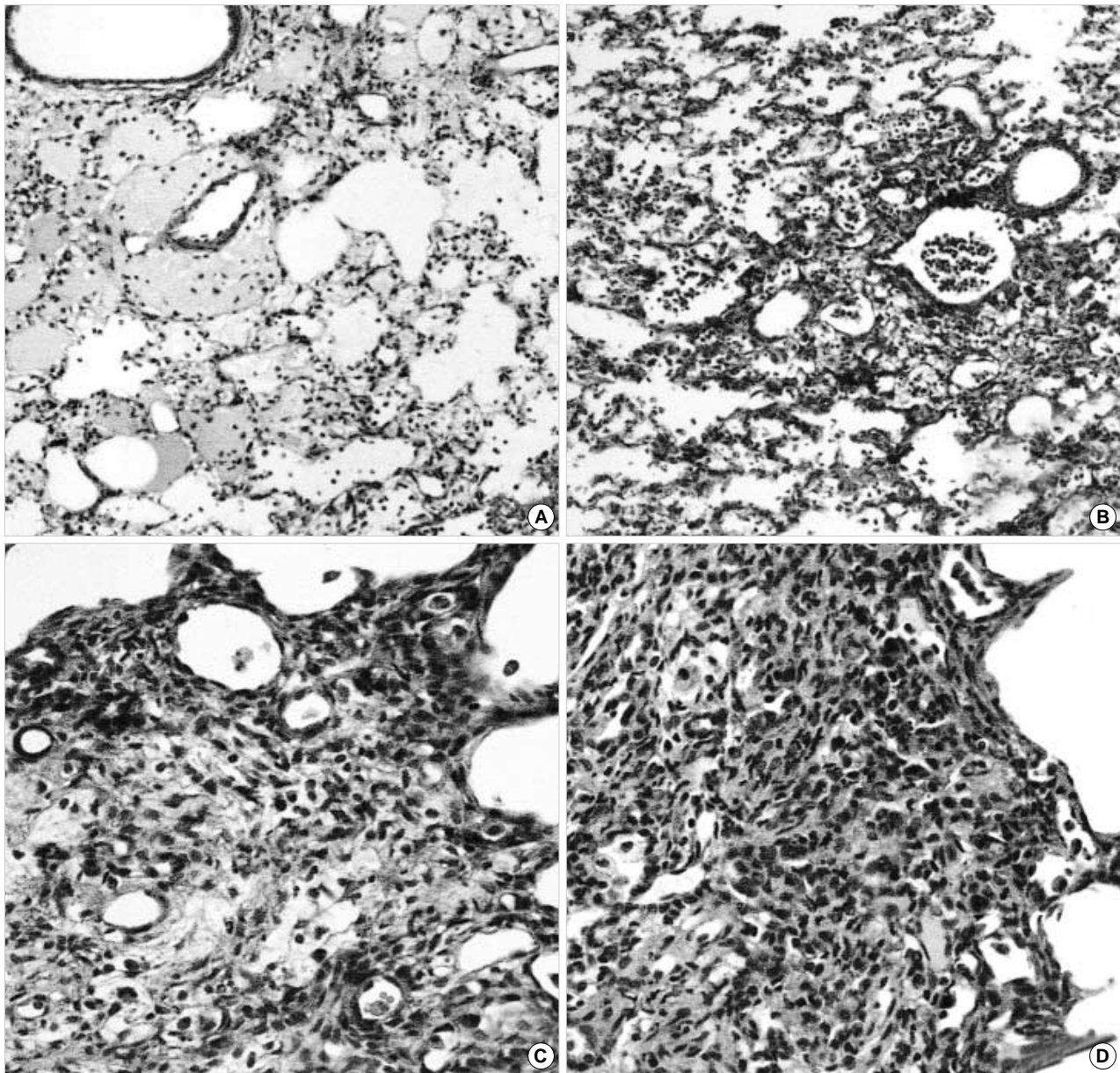


Fig. 1. Light micrograph of the rat lungs after intra-tracheal injection of cadmium. (A) The lung observed on Day 1 after the administration of cadmium shows mild inflammatory infiltrates with partially intra-alveolar edema and fibrin materials. (B) On Day 3, the lung shows patchy inflammatory infiltration in the peribronchiolar portion, intra-alveolar desquamated epithelial cells and fibrin materials. (C) On Day 7, the lung shows multiple patchy peribronchiolar inflammatory consolidations and associated with scattered collagen deposit. (D) On Day 10, the patchy inflammatory consolidation with collagen deposit is more prominent than the change of lungs observed on Day 7 (H&E, Original magnification, A&B: $\times 100$, C&D: $\times 200$).

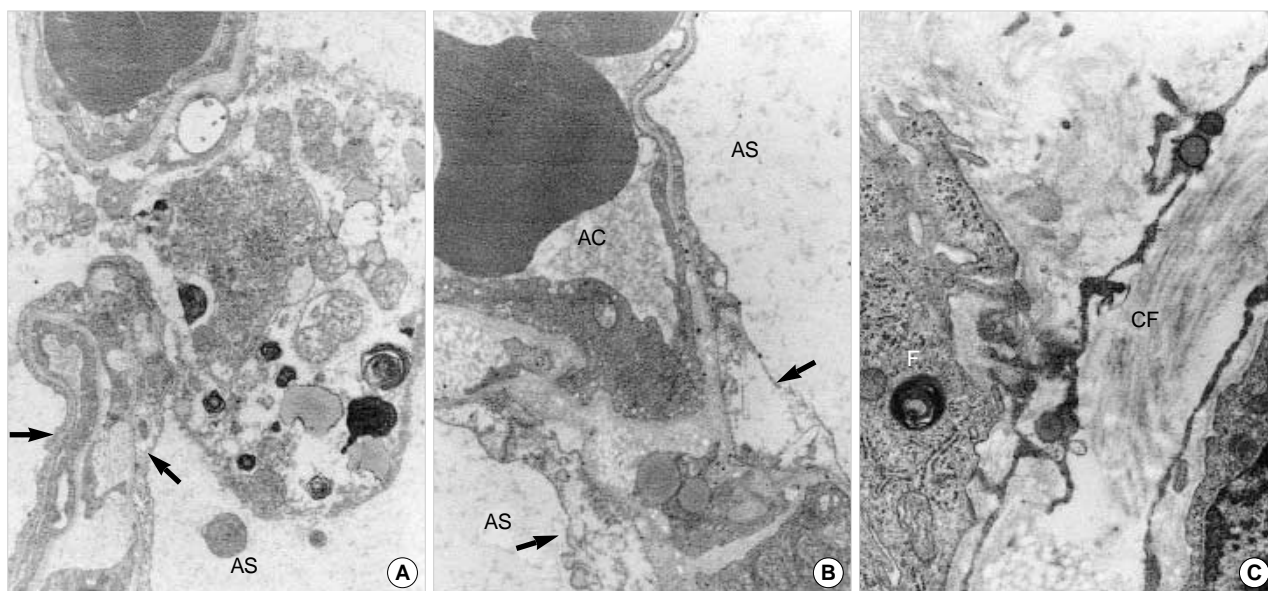


Fig. 2. Transmission electron micrograph of the rat lungs after intra-tracheal injection of cadmium. (A) On Day 1, the alveoli show focal collapse (arrows), swelling of type I epithelial cells, intra-alveolar fibrin materials, and desquamated epithelial debris. (B) On Day 3, the lung shows edematous alveolar wall thickening and swelling of the alveolar type I cells (arrows). (C) On Day 10, the lung parenchyma shows some fibroblast proliferation (F) and interstitial deposit of collagen fibrils (CF) in the alveolar wall. AC: alveolar capillary, AS: alveolar space. Original magnification, A: $\times 5,000$, B: $\times 5,000$, C: $\times 8,000$.

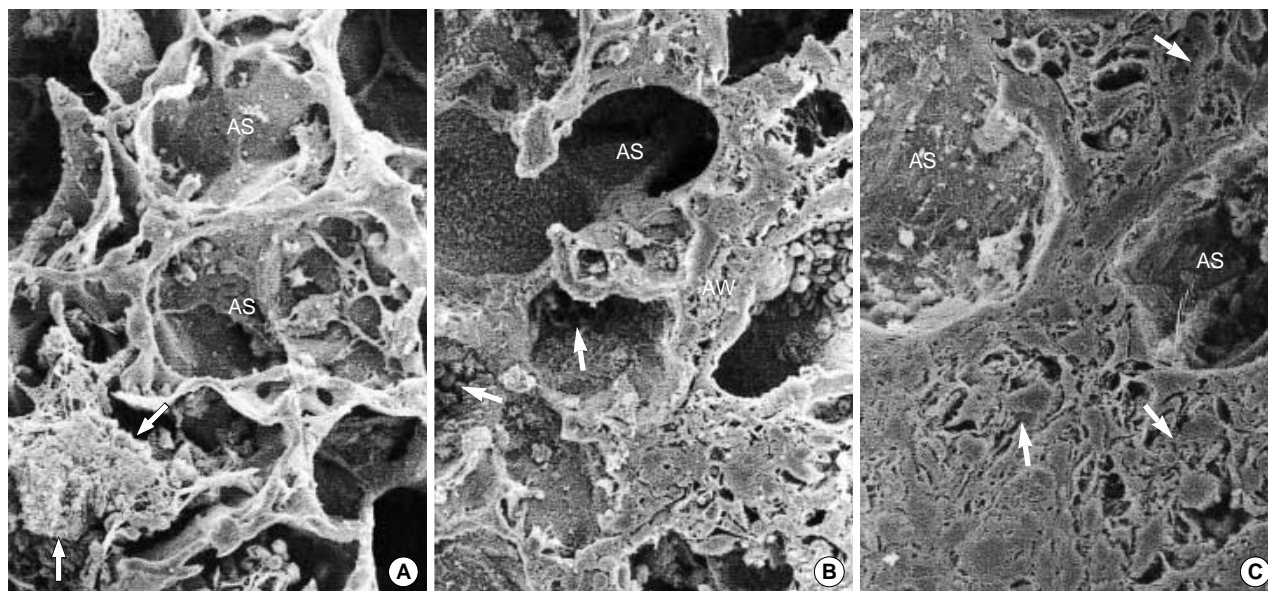


Fig. 3. Scanning electron micrograph of the rat lungs after intra-tracheal injection of cadmium. (A) On Day 1, the alveoli show focal collapse, intra-alveolar fibrin materials, and desquamated epithelial debris (arrows). (B) On Day 3, the lungs show alteration of the alveolar architecture, irregular thickening of alveolar walls, and some intra-alveolar destroyed materials (arrows). (C) On Day 7, the alveoli show irregular dilatation and consolidation with fibroblastic proliferation (arrows). AS: alveolar space, AW: alveolar wall. Original magnification, A: $\times 300$, B: $\times 300$, C: $\times 600$.

chiolar lumina. On Day 10 after the injection of cadmium, the inflammatory lesion was subsided, but a few patchy lesions with more fibrotic consolidation were seen around the bronchiolar regions (Fig. 1).

Electron microscopic examination

Transmission and scanning electron microscopically, on Day 1 after the injection of cadmium, the alveoli were focally collapsed, swelling of type I epithelial cells, intra-alveolar fibrin

materials and desquamated epithelial debris. On Day 3 after the injection of cadmium, the lungs showed multifocally irregular alteration of the alveolar architecture, edema of the alveolar walls and intra-alveolar destroyed materials. The alveoli showed lining of plump type II cells, and contained some fibrin materials. The alveolar walls showed inflammatory cells and some scattered collagen fibrils. On Day 7, the alveoli regained a normal architecture, but in part, the alveolar structures were still collapsed or irregularly dilated. Areas of some fibroblastic proliferation with collagen fibrils were noted in the alveolar walls. The areas with deposition of collagen fibrils were more prominent on Day 10 after cadmium injection (Fig. 2, 3).

Light microscopic TUNEL expression

The TUNEL stains from the dry ice-acetone frozen tissue revealed that the proportion of the apoptotic respiratory cells was 11.8% on Day 1, 2.8% on Day 3, 0.9% on Day 7, and 0.5% on days 10. The TUNEL stains from the formalin-fixed paraffin embedded tissue revealed that the proportion of apop-

totic respiratory cells was 7.0% on day 1, and 1.0% on Day 3, 0.3% on days 7, and 0.1% on Day 10 (Fig. 4). The apoptosis of respiratory cells was most prominent on Day 1 after

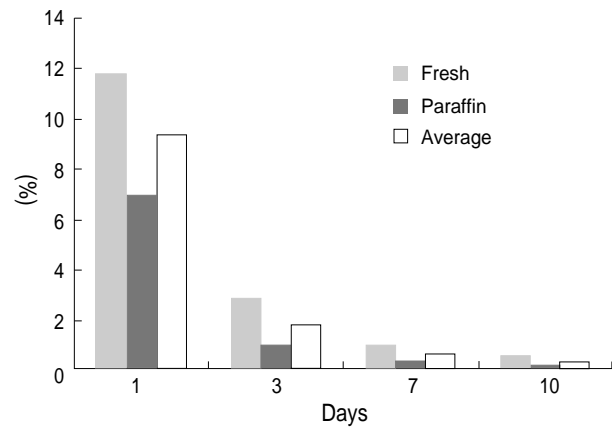


Fig. 4. Positive expression rate of respiratory epithelial cells in light microscopic TUNEL stain at the times after intra-tracheal cadmium injection. Fresh: freshly frozen lung tissue, Paraffin: paraffin-embedded lung tissue.

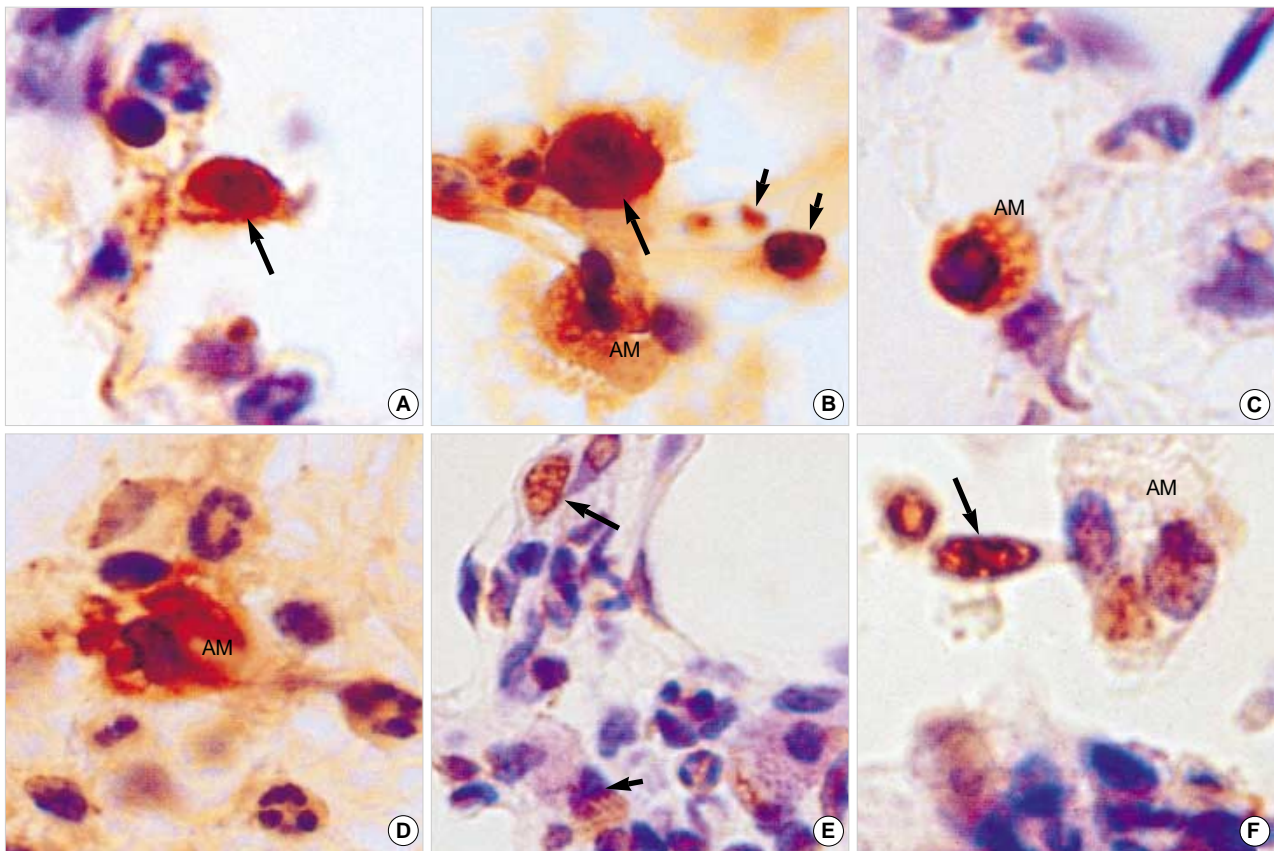


Fig. 5. Light microscopic TUNEL expression in the rat lung tissues. (A) to (C) On Days 1 and 3 after the administration of cadmium. The TUNEL stains show positive expression of alveolar epithelial cells (long arrows), apoptotic bodies (short arrows), and cytoplasmic expression of the alveolar macrophages (AM). Original magnification, (A) to (C) $\times 600$. D to F: On Days 7 and 10 after the administration of cadmium. The alveolar macrophages show positive TUNEL expressions in the cytoplasm (AM). Some spindle shaped cells (long arrows) and inflammatory cells (short arrow) show positive TUNEL expression. Original magnification, (A&F) $\times 600$, E: $\times 400$.

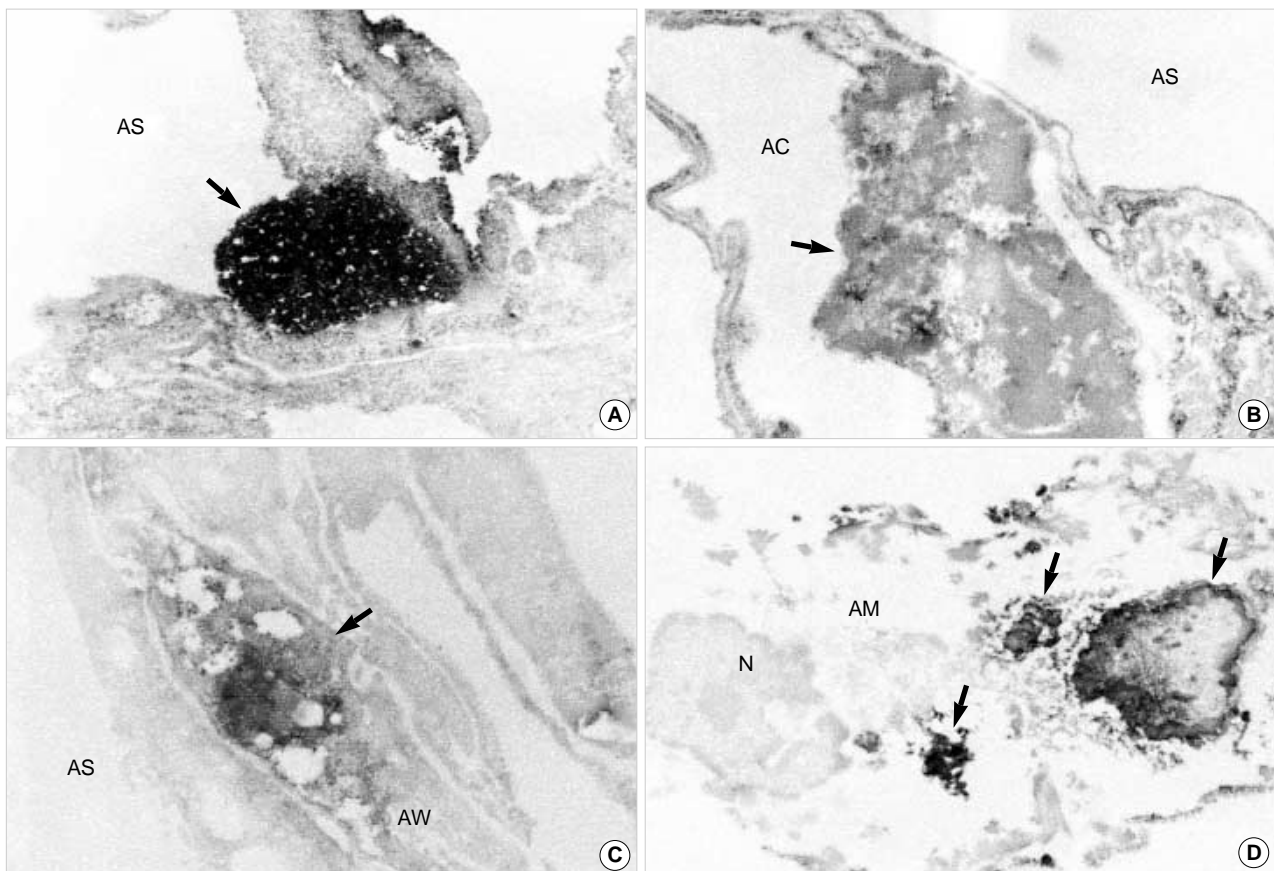


Fig. 6. Electron microscopic TUNEL stains show an electron dense, homogeneous expression of the apoptotic nuclei (arrows) in the alveolar epithelial cell (A), alveolar endothelial cell (B), and interstitial cell of the alveolar wall (C). The alveolar macrophage contains electron-dense expressed apoptotic nucleus and nuclear fragments in the cytoplasm (arrows) (D). The nucleus of the alveolar macrophage (N) is negative for the TUNEL stain. AC: alveolar capillary, AM: alveolar macrophage, AS: alveolar space, AW: alveolar wall. Original magnification, A: $\times 9,000$, B: $\times 6,000$, C: $\times 9,000$, D: $\times 6,000$.

the injection of cadmium, and then the number of apoptosis was markedly decreased on Days 3 and 7. After Day 7, the alveolar macrophages and some epithelial cells or interstitial cells showed frequent phagocytosis of apoptotic bodies or apoptotic debris. The neutrophils in the patchy lesions showed apoptosis on the sections of Days 7 and 10 (Fig. 5). Generally, the apoptotic cells showed cell shrinkage, detachment from their neighbor cells, cytoplasmic condensation, and fragmentation of the nuclei into multiple apoptotic nuclear bodies. The apoptotic cells occasionally did not well clarify the morphologic nature on the light microscopic TUNEL stain.

Electron microscopic TUNEL expression

On Day 1 after the injection of cadmium, the respiratory epithelial cells, some alveolar endothelial cells, interstitial cells and alveolar macrophages showed positive TUNEL expressions in the various stages of nuclear apoptosis (Fig. 6). The nuclear chromatin of the apoptotic cells are frequently fragmented and compacted into irregularly delineated masses that lie

against the nuclear envelope. The early stage of nuclear apoptosis showed electron dense expression mostly around the inner nuclear membranes. The next stages of apoptotic nuclei showed round to oval configuration with more diffuse and homogenous electron dense expression, formation of some intra-nuclear blebs and buddings which protrude to outside of the nuclear membranes, and separation into multiple apoptotic nuclear bodies or apoptotic debris (Fig. 7). On Days 3 and 7, the numbers of TUNEL positive nuclear expression were markedly decreased. On Day 10, TUNEL positive apoptotic nuclear bodies or nuclear debris were observed in the cytoplasm of the alveolar macrophages, and occasionally adjacent respiratory epithelial cells or interstitial cells (Fig. 6).

DISCUSSION

It is well known that inhaled cadmium can cause clinically pneumonitis, pulmonary emphysema, and occasionally acute lung injury (3). The exposure of lung to cadmium causes the

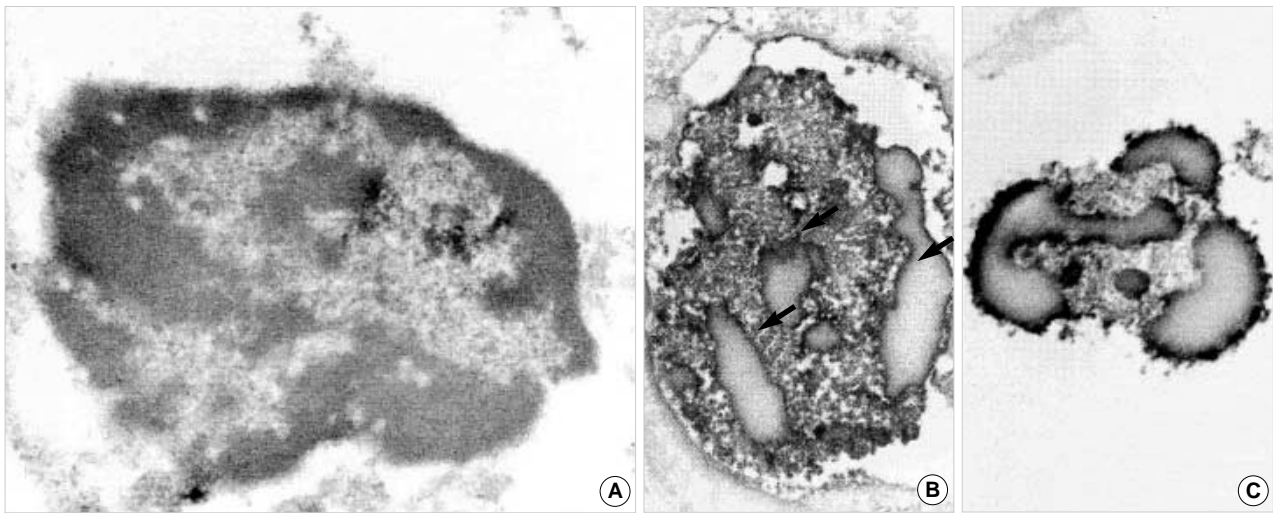


Fig. 7. Electron microscopic TUNEL stains show different morphologic expression of the nuclear apoptosis. (A) An early apoptotic nucleus with electron dense expression along the nuclear membrane. (B) An apoptotic nucleus with electron dense expression and several intra-nuclear blebs (arrows). (C) The apoptotic nuclei are separated, and form the apoptotic nuclear bodies. Original magnification, A: $\times 24,000$, B: $\times 12,000$, C: $\times 11,000$.

alterations of cellular function, and in addition, leads to a complex series of events. It also results in death of the cells, and in two fundamentally different forms of necrosis and apoptosis (14). The mechanisms were not clearly defined, but an oxidative stress response might play an early role in promoting cadmium-induced apoptosis in the lung epithelial cells (14, 15).

The programmed cell death, apoptosis was first introduced by Kerr et al. (16), and was described as a form of cell death with well-defined morphological features and controlled cleavage of DNA (17, 18). On the electron microscopic examination, the apoptotic cells illustrate characteristically condensed nuclear chromatin, often into a crescent-shaped mass aggregated onto the inner surface of the nuclear envelop and frequently fragmentation. In the cytoplasm, the ground substance also becomes condensed, and leads to shrinkage of the cytoplasm (19, 20). The mitochondria retain their integrity until relatively late in the apoptotic process. Eventually cytoplasmic bleb occurs, and membrane-bound bodies are pinched off from the cytoplasm (apoptotic bodies), which are phagocytosed by the alveolar macrophages or the neighbor cells (21).

In this study, the electron microscopic TUNEL stain illustrated the various morphologic features of nuclear expression in the apoptotic respiratory cells. The apoptotic nuclei revealed electron dense expression of chromatins under inner nuclear membranes, more diffuse and homogenous, and round to oval electron dense expression. Frequently apoptotic nuclei revealed the intra-nuclear blebs and occasionally protrusion to outside of nuclei, and eventually separation into multiple apoptotic nuclear bodies or apoptotic debris which were phagocytosed by the alveolar macrophages or neighboring respiratory parenchymal cells. The findings of intra-nuclear blebbing and projection to the outside of nuclei were not described in the

other literatures. When alveolar macrophages phagocytized the aged apoptotic cells during apoptosis, the apoptotic cell membranes are still intact or disrupted, and we could observe several TUNEL positive apoptotic nuclear bodies or debris in the alveolar macrophages.

The TUNEL method is generally used for in situ labeling of the DNA strand breaking that occurs in the individual nuclei of the apoptotic cells (22). The TUNEL expression is based on the observation that the early stages of apoptosis typically involve the cleavage of chromatin (22). The principle of TUNEL method is that the TdT to specifically bind at exposed 3'-OH terminal of double- or single-stranded DNA fragments, and synthesize a labeled polydeoxynucleotide by incorporation of modified deoxyuridine (X-dUTP, X=biotin, digoxigenin, or fluorescein) into the sites of DNA cleavage. The signal is then enhanced by streptavidin or antidigoxigenin antibody peroxidase and can be detected using DAB (13, 22, 23). The digoxigenin-antidigoxigenin labeling system has been shown to produce lower background staining than other systems and to yield more intense signal in apoptotic cells than non-apoptotic cells, including necrotic cells (24, 25). Using TUNEL method, we could detect the DNA fragmentation in the morphologically intact cells, as well as histologically defined apoptotic cells at early stages of the apoptosis.

Morphologically, the apoptotic cells are not always easily differentiated from necrotic cells on routine light microscopic or electron microscopic examination. The TUNEL stain can detect the apoptotic cells from the necrotic cells and morphologically intact cells (26). On the electron microscopic TUNEL stain, we could identify the nature of apoptotic cells, and examine the detail morphology of various stages of nuclear apoptosis which could not be examined on the light microscopic

TUNEL stain. The early stage of nuclear apoptosis appeared to be associated with faint positive expression on the inner nuclear chromatin portion of somewhat wrinkled nuclei. The faint positive expression of the early nuclear apoptosis, however, might be equivocal in interpretation.

In our results of the cadmium-induced acute lung injury, the apoptosis of respiratory epithelial cells was most prominent on Day 1, and then markedly decreased on Days 3 and 7. The phagocytosis of the apoptotic respiratory cells and inflammatory cells including neutrophils were more prominent on Days 7 and 10 than those of Days 1 and 3 after the injection of cadmium. These findings indicate that apoptosis of the respiratory epithelial cells occurred in the early time after the injection of cadmium, and followed by phagocytosis of the apoptotic cells by the alveolar macrophages or neighboring cells. The phagocytic cells contribute to the clearance of apoptotic respiratory cells and neutrophils from the lesions of acute lung injury.

REFERENCES

1. Milligan CE, Schwartz LM. Programmed cell death during animal development. *Br Med Bull* 1997; 52: 570-90.
2. Hets SW. To die or not to die: An overview of apoptosis and its role in disease. *JAMA* 1998; 279: 300-7.
3. Paterson JC. Studies on the toxicity of inhaled cadmium. III The pathology of cadmium smoke poisoning in man and in experimental animals. *J Industr Hyg Toxicol* 1947; 29: 294-301.
4. Lin CJ, Yang PC, Hsu MT, Yew FH, Liu TY, Shun CT, Tyan SW, Lee TC. Induction of pulmonary fibrosis in organ-cultured rat lung by cadmium chloride and transforming growth factor- β 1. *Toxicology* 1998; 127: 157-66.
5. Driscoll KE, Maurer JK, Poynter J, Higgins J, Asquith T, Miller NS. Stimulation of rat alveolar macrophage fibronectin release in a cadmium chloride model of lung injury and fibrosis. *Toxicol Appl Pharmacol* 1992; 116: 30-7.
6. El Azzouzi B, Tsangaris G, Pellegrin O, Manuel Y, Benveniste J, Thomas Y. Cadmium induces apoptosis in a human T cell line. *Toxicology* 1994; 88: 127-39.
7. Tsangaris GT, Tzortzidou-Stathopoulou F. Cadmium induces apoptosis differentially on immune system cell lines. *Toxicology* 1998; 128: 143-50.
8. Ishido M, Homma ST, Leung PS, Tohyama C. Cadmium-induced DNA fragmentation is inhibitable by zinc in porcine kidney LLC-PK1 cells. *Life Sci* 1995; 56: 351-6.
9. Tanimoto A, Hamada T, Koide O. Cell death and regeneration of renal proximal tubular cells in rats with subchronic cadmium intoxication. *Toxicol Pathol* 1993; 21: 341-52.
10. Xu C, Johnson JE, Singh PK, Jones MM, Yan H, Carter CE. *In vivo studies of cadmium-induced apoptosis in testicular tissue of the rat and its modulation by a chelating agent. Toxicology* 1996; 107: 1-8.
11. Habeebu SSM, Liu J, Klaassen CD. Cadmium-induced apoptosis in mouse liver. *Toxicol Appl Pharmacol* 1998; 149: 203-9.
12. Bell RR, Nonavinakere VK, Soliman MRI. Intratracheal exposure of the guinea pig lung to cadmium and/or selenium: a histological evaluation. *Toxicol Lett* 2000; 114: 101-9.
13. Ansari B, Coates PJ, Greenstein BD, Hall PA. *In situ end labeling detects DNA strand breaks in apoptosis and others physiological and pathological states. J Pathol* 1993; 170: 1-8.
14. Hart BA, Lee CH, Shukla GS, Shukla A, Osier M, Eneman JD, Chiu JF. Characterization of cadmium-induced apoptosis in rat lung epithelial cells; evidence for the participation of oxidant stress. *Toxicology* 1999; 133: 43-58.
15. Payne CM, Bernstein C, Bernstein H. Apoptosis overview emphasizing the role of oxidative stress, DNA damage, and signal-transduction pathways. *Leukemia & Lymphoma* 1995; 19: 43-93.
16. Kerr JFR, Wyllie AH, Currie AR. Apoptosis: a basic biological phenomenon with wide-ranging implications in tissue kinetics. *Br J Cancer* 1972; 25: 239-45.
17. Compton MM. A biochemical hallmark of apoptosis, internucleosomal degradation of the genome. *Cancer Metast Rev* 1992; 11: 105-19.
18. Gerschenson LE, Rotello RJ. Apoptosis: a different types of cell death. *FASEB J* 1992; 6: 2450-5.
19. Kerr JFR. Shrinkage necrosis, a distinct mode of cellular death. *J Pathol* 1971; 105: 13-20.
20. Wyllie AH. Cell death: a new classification separating apoptosis from necrosis. In: *Cell death in biology and pathology*. London, Chapman and Hall, 1981; 9-34.
21. Sanders EJ. Methods for detecting apoptotic cells in tissues. *Histol Histopathol* 1997; 12: 1169-77.
22. Valavanis C: *In situ detection of dying cells in normal and pathological tissues*. In Schwartz LM, Ashwell JD (Eds): *Apoptosis*. London, Academic press, 2001; 393-415.
23. Gavrieli Y, Sherman Y, Ben-Saaon SA. Identification of programmed cell death in situ via specific labeling of nuclear DNA fragmentation. *J Cell Biol* 1992; 119: 493-501.
24. Gorczyca W, Bigman K, Mittelman A, Ahmet T, Gong J, Melamed MR, Darzynkiewicz Z. Induction of DNA strand breaks associated with apoptosis during treatment of leukemias. *Leukemia* 1993; 7: 659-70.
25. Li X, James WM, Traganos F, Darzynkiewicz Z. Application of biotin, digoxigenin, or fluorescein-conjugated deoxynucleotides to label DNA strand breaks in analysis of cell proliferation and apoptosis using flow cytometry. *Biotech Histochem* 1995; 70: 234-42.
26. Mesner PW, Kauffman SH. Methods utilized in the study of apoptosis. *Adv Pharmacol* 1997; 41: 57-87.